

Electronic Supplementary Information

**Efficient photocatalytic Suzuki cross-coupling reactions on Au-Pd alloy nanoparticles under visible light irradiation**

Qi Xiao,<sup>a</sup> Sarina Sarina,<sup>a</sup> Esa Jaatinen,<sup>a</sup> Jianfeng Jia,<sup>a</sup> Dennis P. Arnold,<sup>a</sup> Hongwei Liu,<sup>a</sup> and Huaiyong Zhu <sup>a\*</sup>

<sup>a</sup> School of Chemistry, Physics and Mechanical Engineering, Faculty of Science and Technology, Queensland University of Technology, Brisbane, QLD 4001, Australia.

E-mail: hy.zhu@qut.edu.au; Fax: +61 7 3138 1804; Tel: +61 7 3138 1581.

**LEGENDS**

**Figure S1.** Absorption intensity of Au-Pd alloy NPs on ZrO<sub>2</sub> and irradiation intensity of incandescent light (including the calculation method of quantum yield)

**Figure S2.** The wavelength range of the high intensity LED

**Figure S3.** The geometries of iodobenzene molecule and iodobenzene negative ion based on DFT calculation

**Figure S4.** The optimized geometry and the natural charge distributions of the Au<sub>32</sub> cluster and Au<sub>12</sub>Pd<sub>20</sub> clusters in ground state and considered excited state

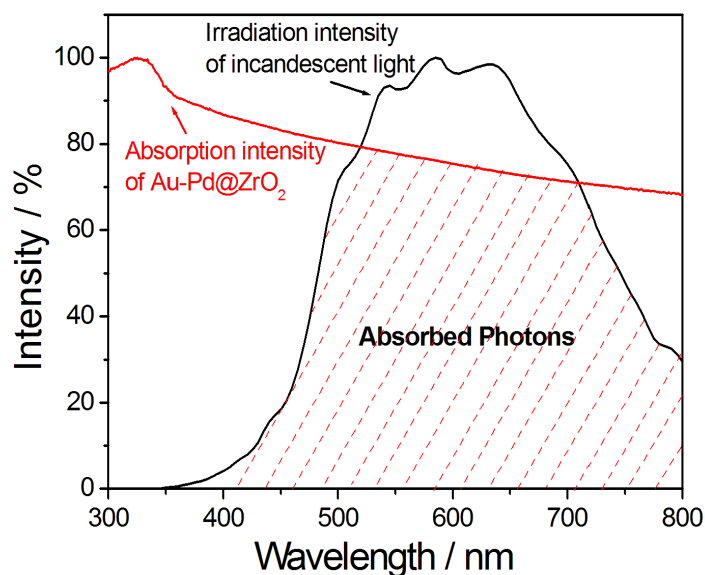
**Figure S5.** Comparison of the results for the reactions interrupted at 0.5 h and 1.0 h

**Text S1.** Estimation of Au-Pd alloy NPs' ionic property by free gas model

**Text S2.** DFT calculation of charge distribution in Au-Pd alloy nanoparticle.

**Figure S1.**

Absorption intensity of Au-Pd alloy NPs on ZrO<sub>2</sub> (red curve) and irradiation intensity of incandescent light (black curve). The overlapped area indicates the distribution of the absorbed photons.



The calculation method of quantum yield:

The light intensity measured at the reaction system was 0.50 W/cm<sup>2</sup> (which included both the absorbed and scattered light). The overall energy of the photons of the irradiation on the reaction system was derived from the product of the light intensity and section area of the reactor, which under irradiation. The overlap of the light source and the absorption spectrum of catalysts provide the distribution of the absorbed photons over the wavelength range between 400 nm and 800 nm, as shown in the figure. We could estimate the mean wavelength of the absorbed photons from the distribution (after being normalized). The mean energy of the photons could be calculated from the mean wavelength. The number of the photons introduced in the reaction system in our study was calculated from the ratio of the overall energy of the photons and mean energy of the photons. The number of molecules formed was determined by the light induced conversion (calculated by difference of photoreaction and thermal reaction). Thus the apparent quantum yield was from the ratio of the number of molecules formed to the number of the photons introduced in the reaction system.

**Figure S2.**

The wavelength range of the high intensity LED.

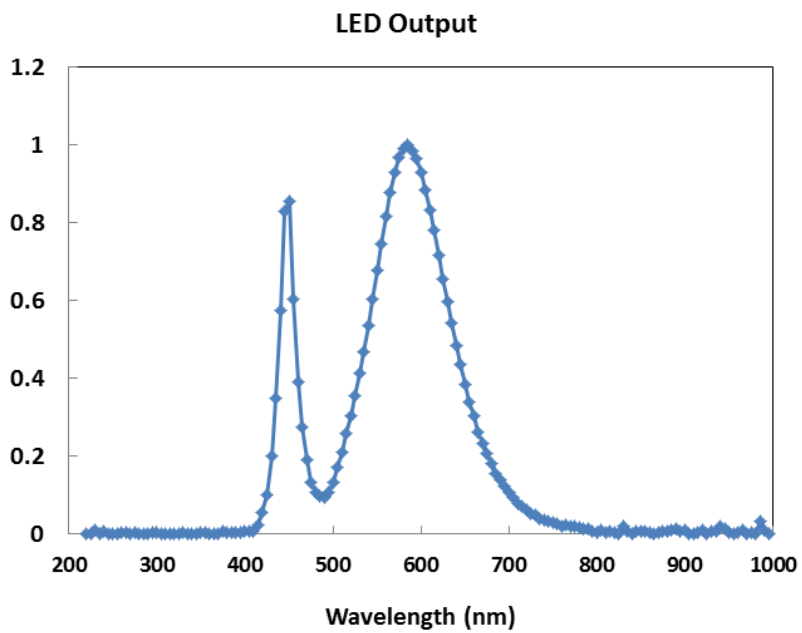


**Figure S3.**

The geometries of iodobenzene molecule (left) and iodobenzene negative ion (right) (bond length in Å). Detailed DFT calculation method, see Supplementary Text below.

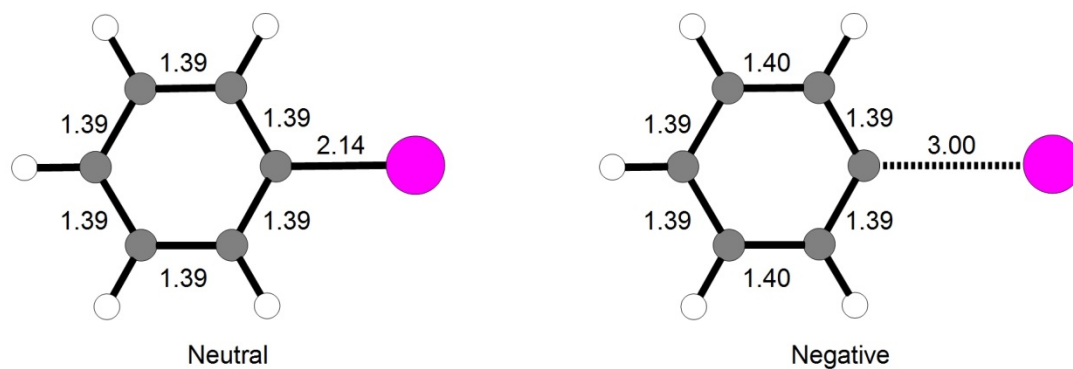


**Figure S4.**

The optimized geometry and the natural charge distributions of the Au<sub>32</sub> cluster (A) and Au<sub>12</sub>Pd<sub>20</sub> clusters (B) in ground state and considered excited state.

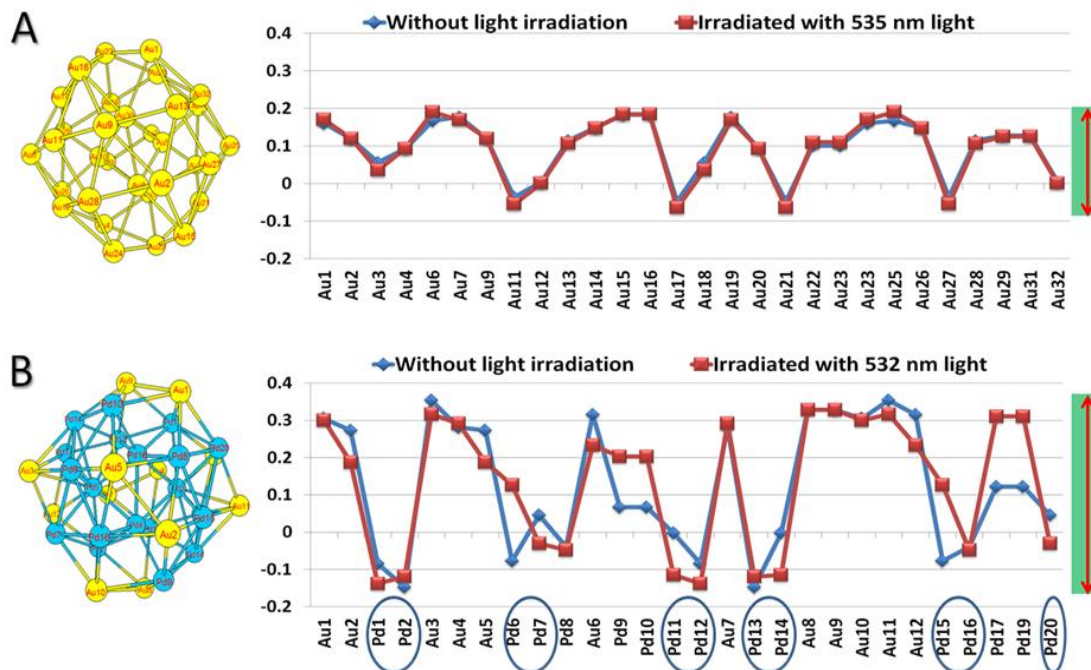
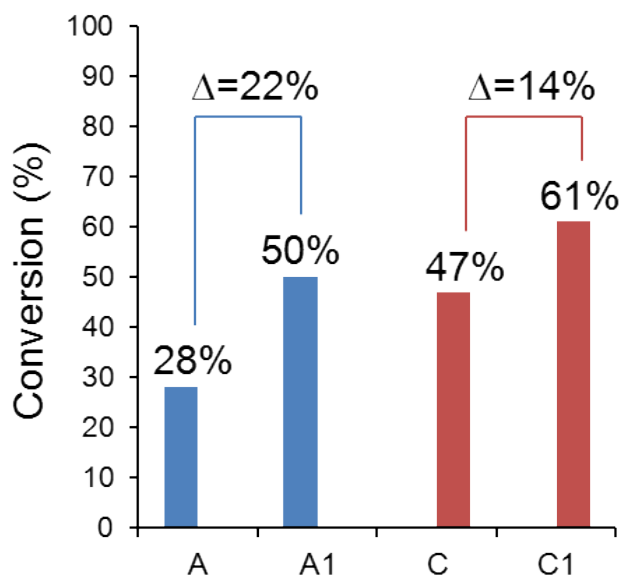


**Figure S5.**

Comparison of the results for the reactions interrupted at 0.5 h (A and A1) and 1.0 h (C and C1).

The reaction was interrupted at 1.0 h, and the catalyst was removed by centrifugation, the solution was labelled as C, 0.5 mL sample was collected for GC test. The rest solution without catalyst was re-irradiated as typical procedure, and after the reaction, sample was collected for GC test (labelled as C1). We compared the results with that for the reaction interrupted at 0.5 h (solution A and A1). We can see that after 1.0 h, the reaction proceeded smoothly with catalyst, and the reaction increased from 28 % (A) to 47 % (C). After removing catalyst, the conversion for C1 is 61 %, and the conversion for A1 is 50 %. The difference between A and A1 is 22 %, which is much higher than that between C and C1 (14 %). Thus the catalytic efficiency of the supernatant in 1.0 h is lower than that in 0.5 h, the reaction did not proceed too much for the solution C, which means that less alloy NPs was peeled off after 0.5 h. Moreover, from the reusability of the Au-Pd alloy NPs (Figure 10 in main text), we can also confirm that the catalytic activity doesn't lose too much during the reaction. All of these results can support our conclusion that visible light can stimulate the reaction in the initial phase (within 0.5 h), and the trace of alloy NPs may be peeled off in the supernatant, but overall the main contribution of the activity results from the photocatalytic response of heterogeneous Au-Pd alloy NPs.



### Text S1. Estimation of Au-Pd alloy NPs' ionic property by free gas model.

The electron redistribution of the Au-Pd bond is dependent on the magnitude of the electron transferred between the two metals. An estimate of magnitude of the charge transferred can be obtained with the free electron gas model,<sup>1</sup> with the change in the number of electrons given by:

$$\Delta N = D(\varepsilon_{F,Au})\Delta a = D(\varepsilon_{F,Pd})\Delta b \quad (1)$$

where  $D(\varepsilon_F)$  is the density of electron states at the Fermi energies for the two metals and:

$$\Delta a = \Phi_{Pd} - \Phi^* \quad (2a)$$

$$\Delta b = \Phi^* - \Phi_{Au} \quad (2b)$$

$$\Delta a + \Delta b = \Phi_{Pd} - \Phi_{Au} \quad (2c)$$

where  $\Phi_{Pd}$  and  $\Phi_{Au}$  are the work functions of pure palladium and gold, respectively, and  $\Phi^*$  is the work function of the alloy once charge equilibrium is reached. Effectively  $\Delta a$  and  $\Delta b$  give the shift in Fermi level (chemical potential) of the two metals at their interface upon contact. The density of states of a free electron gas at the Fermi level<sup>2</sup> is given by (3):

$$D(\varepsilon_F) = \frac{3N}{2\varepsilon_F} \quad (3)$$

where  $N$  is the number of electrons, so for the two metals the densities are:

$$D(\varepsilon_{F,Au}) = \frac{3N_{Au}}{2\varepsilon_{F,Au}} \quad (3a)$$

$$D(\varepsilon_{F,Pd}) = \frac{3N_{Pd}}{2\varepsilon_{F,Pd}} \quad (3b)$$

Combining Equations 3a and 3b with Equation 1 the ratio Fermi level shift is given by:

$$\frac{\Delta a}{\Delta b} = \frac{N_{Pd}}{N_{Au}} \frac{\varepsilon_{F,Au}}{\varepsilon_{F,Pd}} \quad (4)$$

In the alloy systems in this study, the relative concentration of Pd and Au is varied. If the relative concentration of Pd in the alloy is  $x$ , then that of Au will be  $1-x$  and Equation 4 becomes:

$$\frac{\Delta a}{\Delta b} = \frac{x}{1-x} \frac{\varepsilon_{F,Au}}{\varepsilon_{F,Pd}} \quad (5)$$

By combining Equation 5 with Equations 2c and 1, the total change in electron concentration can be evaluated:

$$\Delta N = \frac{3}{2} \frac{x}{\varepsilon_{F,Pd}} \frac{(\Phi_{Pd} - \Phi_{Au})}{1 + \frac{x}{1-x} \frac{\varepsilon_{F,Au}}{\varepsilon_{F,Pd}}} K = \frac{3}{2} \frac{x}{5.6} \frac{(5.6 - 5.3)}{1 + \frac{x}{1-x} \frac{5.3}{5.6}} K \quad (6)$$

where  $K$  is a constant of proportionality. Therefore, the net increase in electron concentration on the Pd outer-shell of the nanoparticle will be:

$$\Delta N = K' \frac{0.4x}{1 + \frac{x}{1-x} 0.9} \sim 0.4K'x(1-x) \quad (7)$$

A plot of  $\Delta N$  as a function of the gold concentration in the Au-Pd alloy NPs,  $1-x$ , is shown in Figure 6. The maximum charge transfer occurs at approximately  $x = 0.5$  (i.e. Au:Pd ratio of the alloy particles is 1:1).

## References

1. K. Yamada, K. Miyajima, F. Mafun, *J. Phys. Chem. C* **2007**, *111*, 11246-11251.
2. C. Kittel, *Introduction to Solid State Physics*, 8<sup>th</sup> ed. Wiley and Sons, New York, **2005**.

## Text S2. Density function theory (DFT) calculation of charge distribution in Au-Pd alloy nanoparticle.

An Au<sub>32</sub> cluster and a corresponding Au<sub>12</sub>Pd<sub>20</sub> alloy cluster were constructed to mimic the Au and Au-Pd nanoparticles. The geometry of the Au<sub>32</sub> and Au<sub>12</sub>Pd<sub>20</sub> were optimized by PBE<sup>1</sup> method of density functional theory implemented in CP2K<sup>2</sup> code. The Molecular optimized double zeta-valence Shorter Range basis sets<sup>3</sup> with a polarization function was used to describe the valence orbitals and Goedecker-Teter-HutterPseudo-potential<sup>4</sup> was used to describe the core electrons. The excited state calculations on as optimized structures were performed in the framework of Time-Dependent density functional theory with B3LYP<sup>5,6</sup> functional provided by Gaussian09 package<sup>7</sup>. In this stage, Lanl2dz basis set<sup>8</sup> was selected to describe the atomic orbital of Au and Pd atoms. The excited states with excited wavelength of 534 nm for Au<sub>32</sub> and 532 nm for Au<sub>12</sub>Pd<sub>20</sub> were considered in our calculations. The optimized geometry of the Au<sub>32</sub> and Au<sub>12</sub>Pd<sub>20</sub> clusters and the natural charge distributions<sup>9</sup> of them in ground state and considered excited state were depicted in Figure S4.

## References

1. Perdew, J. P; Burke, K; Ernzerhof, M., *Physical Review Letters*, 77 (18), 3865-3868 (1996).
2. CP2K version 2.4, the CP2K developers group (2013), <http://www.cp2k.org/>.
3. D. Becke, Density-functional thermochemistry. III. The role of exact exchange, *J. Chem. Phys.* **1993**, 98, 5648-5652.
4. VandeVondele, J; Hutter, J. *J. Chem. Phys.*, 127 (11), 114105 (2007).
5. Krack, M., *Theoretical Chemistry Accounts*, 114 (1-3), 145-152 (2005).
6. Lee, C., Yang, W., and Parr, R. G., *Phys. Rev. B*, **1998**, 3, 785-789.
7. Hay, P. J. and Wadt, W. R., *J. Chem. Phys.* **1985**, 82, 299-310.
8. Frisch, M. J., Trucks, G. W., Schlegel, H. B., G. E. Scuseria, M. A. Robb, J. R. Cheeseman, G. Scalmani, V. Barone, B. Mennucci, G. A. Petersson, H. Nakatsuji, M. Caricato, X. Li, H. P. Hratchian, A. F. Izmaylov, J. Bloino, G. Zheng, J. L. Sonnenberg, M. Hada, M. Ehara, K. Toyota, R. Fukuda, J. Hasegawa, M. Ishida, T. Nakajima, Y. Honda, O. Kitao, H. Nakai, T. Vreven, J. A. Montgomery, Jr., J. E. Peralta, F. Ogliaro, M. Bearpark, J. J. Heyd, E. Brothers, K. N. Kudin, V. N. Staroverov, R. Kobayashi, J. Normand, K. Raghavachari, A. Rendell, J. C. Burant, S. S. Iyengar, J. Tomasi, M. Cossi, N. Rega, J. M. Millam, M. Klene, J. E. Knox, J. B. Cross, V. Bakken, C. Adamo, J.

- Jaramillo, R. Gomperts, R. E. Stratmann, O. Yazyev, A. J. Austin, R. Cammi, C. Pomelli, J. W. Ochterski, R. L. Martin, K. Morokuma, V. G. Zakrzewski, G. A. Voth, P. Salvador, J. J. Dannenberg, S. Dapprich, A. D. Daniels, O. Farkas, J. B. Foresman, J. V. Ortiz, J. Cioslowski, and D. J. Fox, Gaussian 09, Revision C.01, Gaussian, Inc., Wallingford CT, 2010.
9. Reed, A. E., Weinstock, R. B., and Weinhold, F., *J. Chem. Phys.*, **83** (1985) 735-46.